Published in final edited form as:
Biochimie. 2014 October ; 0: 99–109. doi:10.1016/j.biochi.2014.06.019.

Sphingolipids and Ceramides of Mouse Aqueous Humor: Comparative Profiles from Normotensive and Hypertensive DBA/2J Mice

Genea Edwards[a], **Katyayini Aribindi**[a], **Yenifer Guerra**[a], and **Sanjoy K. Bhattacharya**[a,*]
[a]Bascom Palmer Eye Institute, University of Miami School of Medicine, Miami, Florida, 33136

Abstract

Purpose—To identify the sphingolipid and ceramide species and their quantitative differences between normotensive and hypertensive intraocular pressure states in DBA/2J mouse aqueous humor (AH).

Methods—Normotensive and hypertensive AH was sampled from mice by paracentesis. Lipid extraction was performed using modifications of the Bligh and Dyer method. Protein concentration was estimated using the Bradford colorimetric assay. Sphingolipids and ceramides were identified and subjected to ratiometric quantification using appropriate class specific lipid standards on a TSQ Quantum Access Max triple quadrupole mass spectrometer.

Results—The comparative profiles of normotensive and hypertensive DBA/2J mouse AH showed several species of sphingomyelin, sphingoid base, sphingoid base-1-phosphate (S1P) and ceramides common between them. A number of unique lipids in each of the above lipid classes were also identified in normotensive AH that were absent in hypertensive AH and vice versa.

Conclusion—A number of sphingolipid and ceramide species were found to be uniquely present in normotensive, but absent in hypertensive AH and vice versa. Further pursuit of these findings is likely to contribute towards expanding our understanding of the molecular changes associated with increased intraocular pressure (IOP) and glaucoma.

Keywords

sphingolipids; ceramides; normotensive; hypertensive; aqueous humor; mass spectrometry

*Corresponding Author: McKnight Vision Research Building, Bascom Palmer Eye Institute, University of Miami Miller School of Medicine, 1638 NW 10th Avenue, Room 706A, Miami, Florida 33136, Tel: 305-482-4103, Fax: 305-326-6547, Sbhattacharya@med.miami.edu.

Disclosures
Authors declare no conflicts of interest.

1. Introduction

Aqueous humor (AH) is the clear liquid that bathes the anterior eye chamber, that is, the region between the lens and the cornea [1]. Experimentally, AH has been shown to be generated in the ciliary body [2, 3]. However, whether all constituent components of AH are generated in the ciliary body or are also contributed by other tissues remains uncertain. Generation and exit of AH has great importance for the health of the anterior eye chamber. The impeded aqueous outflow results in elevated intraocular pressure (IOP), which is the key risk factor [1] to develop glaucoma, a group of irreversibly blinding diseases that affects over 60 million individuals worldwide, rendering it a global health concern [4]. Thus far, the trabecular meshwork (TM), a tiny filter like region in the anterior chamber has received wide attention as the region that confers increased resistance to AH outflow resulting in impeded outflow and elevated IOP in the pathologic state. The TM is constantly bathed in AH. However, whether compositional differences in AH affects health of TM remains to be determined.

Lipids have been found to regulate AH outflow [5, 6]. Prostaglandins (PGs), a single sub-class of lipids found endogenously in the iris and termed irin [7, 8], have been found to significantly increase the AH outflow and reduce IOP [9]. A few non-PG lipids such as lysophosphatidic acid (LPA) and sphingosine-1-phosphate (S1P) also have been found to decrease aqueous humor outflow as well [6]. The precise source of PGs in the anterior eye chamber is still not clear, however, $PGF_{2\alpha}$ analogues have been shown to upregulate the expression of extracellular matrix metalloproteinases (MMPs), which in turn, degrade the extracellular matrix (ECM) of the ciliary muscle. The degradation of the ECM of the ciliary muscle results in less resistance for the AH outflow, thus increasing the outflow through the uveoscleral or unconventional pathway [10]. While the majority of increased drainage due to topical application of PGs is through the uveoscleral outflow pathway, they also incrementally increase the conventional or TM outflow pathway [10, 11]. The different classes of lipids that are present in the AH and their relative amounts in normal AH remains to be investigated [11-13]. Such investigations are the first step towards determination of the sources of each of these constituents in the anterior chamber. Methodological barriers, such as AH being a complex mixture and containing very low amounts of lipids have acted as impediments to detect and quantify the lipids in the AH by most methods thus far. Recent advances in mass spectrometry have largely removed all these methodological barriers [14, 15].

The TM is a dynamic tissue and the surrounding cellular environment, including the compositional material it is bathed in, is expected to change its behavior and dynamic movements [16]. The dynamic movements of TM cells are expected to alter the filtration rate and AH outflow [17, 18]. Sphingolipids are often dynamic constituents of cell membranes playing roles in various signaling processes [19]. Direct interaction with four main classes of target proteins: receptor, effector, enzyme, and transporter proteins influence cellular behavior and function [20]. Sphingolipid modulations has been shown to be associated with response to shear stress [21-23], relevant to TM, which experiences changing shear stress exerted by the flow of aqueous humor upon cellular membranes. Little

is known concerning the roles of sphingolipids and ceramides in the eye, and even less in the AH and its effects on the surrounding tissues, especially TM [11].

Glaucoma pathology resides partly in the transition from ocular normotensive to hypertensive states. DBA/2J mice remains one of the most suitable models that presents a spontaneous elevation in IOP for studying AH composition during the transition from normotensive to hypertensive states. We present here comparative analyses of sphingolipids (sphingomyelin, sphingoid base and S1P species) and ceramides of AH between normotensive and hypertensive states in DBA/2J mice. The metabolism of sphingolipids or cellular enzymatic synthesis of ceramide and other sphingolipids are interlinked as schematically depicted in Fig. 1. We expect the findings presented here will spark investigations, thus providing insight as to what specific role the identified sphingolipids and ceramides might play in the health and biology of the anterior chamber tissues and TM cells in particular.

2. Methods

2.1 Animals

Breeding pairs of DBA/2J mice originally procured from The Jackson Laboratory (Bar Harbor, ME) were maintained at the animal facility/McKnight vivarium at University of Miami Miller School of Medicine. All animal protocols were reviewed and approved by Institutional Animal Care and Use Committee (IACUC) and in accordance with the ARVO statement for use of animals in ophthalmic and vision research. Mice gender and ages used are as indicated in individual experiments with an n=40 for each time point unless stated otherwise. IOP measurements were obtained using a TonoLab instrument (Colonial Medical Supplies, NH). Average IOP from two weeks of twice daily measurements were calculated. We considered ~6-7 month old mice as normotensive (IOP ≤15 mm of Hg) and ~8-9 month old mice as hypertensive when carefully measured IOP showed an IOP ≥18mm of Hg at every single measurement. For the normotensive group no single IOP measurement had been >17 mm of Hg and average IOP over two weeks of measurement had been ≤15 mm of Hg. At 8-9 months of age the IOP elevation in DBA/2J mice is asynchronous [24, 25] and thus any mice that showed an IOP <18 mm of Hg at any single point measurement was excluded from the study.

2.2 Aqueous Humor Procurement and Lipid Extraction

Normotensive and hypertensive AH was sampled from the anterior chamber of DBA/2J mice by paracentesis via syringe (catalog no. 7635-01 Hamilton, Reno, Nevada) with a small 33 gauge removable needle (701RN, catalog no. 7803-05 Hamilton, Reno, Nevada), which is a well established procedure. The syringe and needle were rinsed with LC-MS grade water 5 times preceding and following extraction to flush out impurities. To ensure that samples are contamination free, in between the samples, the wash from a syringe was also evaluated using mass spectrometry. Prior to collection, mice were anesthetized with an injection (0.1ml) of ketamine (100mg/kg) and xylazine (9mg/kg) administered intraperitoneally. A drop of tetracaine hydrochloride ophthalmic solution, 0.5% (Bausch & Lomb, USA) was used to anesthetize the ocular surface just prior to sample collection. A

total of ~1-2 μl of AH was collected per animal and used for lipid extraction. The mice were used simultaneously, that is, they were not solely used for these studies. These mice were ultimately euthanized and other parts of ocular tissues were utilized for other investigations. Aqueous humor samples were subjected to lipid extraction using suitable modifications of the Bligh and Dyer extraction method [26]. The lower organic phase containing the extracted lipids was isolated and solvent dried with a Speed-Vac (Model 7810014; Labconco, Kansas City, MO). Samples were subsequently flushed with argon gas to prevent oxidation. Proteins recovered from the corresponding upper aqueous phase were quantified using Bradford's method [27]. In order to ensure extraction efficiency, an external standard (10 picomoles of 1, 2-ditridecanoyl-sn-glycero-3-phosphocholine) was premixed with AH prior to lipid extraction [13, 28]. All extractions and subsequent handling were done using glass vials to avoid contaminating impurities.

2.3 Mass Spectrometric Analysis

All four classes of sphingolipids (sphingomyelin, sphingoid base and S1P) and ceramide species were analyzed on a TSQ Quantum Access Max (Thermo Fisher Scientific, Pittsburgh, PA) triple quadrupole mass spectrometer controlled using vendor supplied XCalibur software. Extracted lipids were dried and resuspended in LC-MS grade Acetonitrile:Isopropanol (1:1). Samples were infused with a flow rate of 300nl/min and analyzed for 2.00 minute with a 0.500 second scan. The infusions were performed with Triversa Nanomate (Advion Inc., Ithaca, NY) and controlled using Chipsoft 8.3.3 version with previously established optimal spray parameters for each lipid class [15]. Sphingomyelin and sphingoid base sprays were performed in positive ion mode with voltage of 1.55 kV and gas pressure of 0.45 psi; S1P and ceramide in negative ion mode with voltage of 1.3 kV and gas pressure of 0.6 psi. Scans typically ranged from 200 m/z to 1000 m/z unless specified otherwise [11]. A full width at half maximum (FWHM) was set at 0.7 and collision gas pressure was set at 1mTorr. Sheath gas (nitrogen) was set to 20 arbitrary units. Auxiliary gas (Argon) was set to 5 arbitrary units. The collision energy, ion mode, scan mode (precursor ion or neutral loss) and other parameters (Table 1) were set according to previous studies for the specific class of lipid analyzed [11, 15, 29]. Quantification utilized class specific lipid standards [11], all procured from Avanti Polar Lipids, Albaster, Alabama (Table 1), in a two step process developed for automated lipid quantification [15, 30]. The most abundant lipid species were quantified in a class specific manner in the first step after isotopic correction (in direct comparison of peak intensities with the added internal standard for each class), which was subsequently used to quantify less abundant species in the second step [14, 29, 30]. Representative spectra from technical repeats (n=10) were manually inspected and selected by two independent observers.

2.4 Data Analysis

Mass spectrometry data was analyzed using MZ mine 2.9 [31] using a database (*.csv format and containing only sphingolipid and ceramide species entities) downloaded from LIPIDMAPS (www.lipidmaps.org) and subjected to ratiometic quantification in two steps [13, 32]. The identified lipids were subjected to analyses for determination of common and unique lipid species using in-house written excel macros [32, 33]. All bar graphs represent the average amount of sphingolipids and ceramides, that is, mean ± standard error of mean

(SEM), statistical analyses by two tailed paired sample t-test (*$p \leq 0.05$) were performed. Amounts of all lipid species considered unique were found to be significantly different from 0.0 by one-sample *t*-test (*$p \leq 0.05$). Selected common lipid species were considered significantly different between normotensive and hypertensive AH if they had a fold change (fc) ≥ 5.0, which has been indicated by asterisks. Fold changes have been expressed as $\log_2$ of ratio of lipid amount in hypertensive to normotensive state.

3. Results

We analyzed AH sphingolipids (sphingomyelin, sphingoid base and S1P) and ceramides of DBA/2J mice, a strain that develop a spontaneous, age-related and progressive glaucoma. Animals for these studies were divided into two groups based on IOP. However, since IOP in DBA/2J mice is associated with age, normotensive (IOP≤15 mm of Hg) mice were slightly younger in age (6-7 months) compared to ocular hypertensive (IOP ≥18 mm of Hg) mice (8-9 months in age). Every mouse was carefully subjected to IOP measurement twice daily for 15 days prior to aqueous collection and excluded from the study if the IOP deviated from the range even at a single point. Normotensive mice did not exceed IOP at any single point >17 mm of Hg and hypertensive mice did not show any decreased IOP of less than 18 mm of Hg (Fig. 2). Female and male DBA/2J mice showed a slight difference in IOP from 3 to 12 months across all ages (Fig. 2) as noted in previous studies [14, 18, 24].

A 23.2% reduction in the total lipid amounts (sphingolipids and ceramides combined) was found in ocular hypertensive compared to normotensive state (Fig. 3A). Sphingomyelin and sphingoid base contributed to most of the overall reduction, 45.1% and 30.1% respectively, while the S1Ps underwent a significant increase (347.7%) followed by ceramides (3.1%) in the ocular hypertensive state (Fig. 3B-E).

We next analyzed normotensive and hypertensive states by further dividing by gender. Females displayed a 28.3% decrease in total sphingolipid species compared to 17.4% in males (Fig. 4A). The total lipids, for all three sphingolipid classes and ceramides, between normotensive and hypertensive states showed some differences between male and females (Fig. 4B), with the exception of S1P and ceramides, the sphingolipids showed higher total amount in the normotensive compared to hypertensive, similar to the trend for total combined lipids (sphingolipids and ceramides).

Quantitative mass spectrometric lipidomic analyses identified 51 unique sphingolipid species between normotensive and hypertensive AH while a total of 86 common sphingolipid species were identified irrespective of gender (Tables 2-3 and Supplementary Tables S1-2) as detailed below. Fold changes (fc) of common sphingolipids and ceramides species between normotensive and hypertensive states have been presented in Fig. 5. A fold change of ≥5 between the two states was considered significant.

3.1 Sphingomyelin Species

Four most frequently found unique sphingomyelin species were present in normotensive AH irrespective of gender (Tables 2-3). There were 13 unique sphingomyelin species identified in hypertensive AH irrespective of gender (Tables 2-3). A total of 23 common

sphingomyelin species between these two states were identified (Fig. 5). Females and males revealed 30 and 28 species found as common, respectively, between normotensive and hypertensive states (Supplementary Tables S1-2).

3.2 Sphingoid base

One unique sphingoid base species was present in normotensive female AH while one most frequently occurred in hypertensive AH irrespective of gender (Tables 2-3). A total of 26 common sphingoid base species were identified between these two states (Fig. 5), and one of the species, iso (4E, 15-methyl-d16:1) sphingosine showed a 6.2 fold change. Female and males showed 28 and 27 species as common, respectively, between normotensive and hypertensive states (Supplementary Tables S1-2).

3.3 Sphingoid base-1-phosphate

Two most frequently found unique S1P species were identified in female normotensive AH (Table 2). There were no unique species identified in hypertensive AH (Tables 2-3). A total of 5 S1P species were common between these two states, of which, C16 sphinganine-1-phosphate and phytosphingosine showed a fold change of 6.0 and 6.7 respectively (Fig. 5). Females and males showed 5 and 6 species found as common, respectively, between normotensive and hypertensive states (Supplementary Tables S1-2).

3.4 Ceramides

There were 10 most frequently found unique ceramide species present in normotensive AH irrespective of gender (Tables 2-3). There were 20 unique ceramide species identified in hypertensive AH irrespective of gender (Tables 2-3). A total of 31 ceramides were common between these two states, with SM (d17:1/24:1) showing a 5.9 fold change. Females and males showed 43 and 40 species identified as common, respectively, between normotensive and hypertensive states (Supplementary Tables S1-2).

4. Discussion

The AH is the clear fluid that bathes the cornea and the rest of the anterior chamber, provides nutrition to these tissues and carries away the excretory materials [1]. The TM has received wide attention as the region of aberrant increased resistance in the pathologic state and has been subjected to compositional analyses [34, 35]. Only scant attention has been paid to whether compositional changes in the AH affects the TM. The primary TM cells when incubated in AH show morphological and biochemical features that are close to their normal physiological state than those grown in serum containing medium [36]. The active ingredients of AH that may contribute to TM cell health remain unknown.

Members of eicosanoid sub-class of lipids, or PGs, increase AH outflow, albeit much more via the uveoscleral than the conventional TM mediated pathway [37]. Recent studies have shown the effect on AH outflow by selected species of others classes of lipids including sphingolipids and ceramides [6, 38, 39]. However, the identification of all lipid species of these classes in the AH remained unknown, which is why we undertook the current mass spectrometric investigation.

Sphingolipids comprise of lipids that can be converted to a variety of species, among them being ceramides, sphingosines, sphingomyelins and S1Ps. The sphingolipids are found in all eukaryotic cell membranes [23, 40, 41]. Sphingolipids are located only in the outer (exoplasmic) leaflet of the plasma membrane bilayer [42], while glycerophospholipids (for example, phosphatidylserine and phosphatidylethanolamine) normally occur only in the inner (cytoplasmic) leaflet. The sphingolipids have gained attention for having significant signaling and regulatory roles within cells, in addition to being structural components of cell membranes [19, 43]. Advances in biochemistry and molecular biology have demonstrated that these lipids play key roles in the regulation of several fundamental biological processes such as signal transduction, cell proliferation, migration, and apoptosis [44]. These regulations are mediated by many enzymes (Fig. 1, Table 4 and Supplementary Table S3) involved in sphingolipid metabolism [45]. The application of specific sphingolipids such as S1P has been known to modulate AH outflow [6, 46].

Shear stress has been shown to induce relocalization of enzymatic proteins that promote sphingolipid synthesis [21]. Several ceramide species have been shown to mimic mechanotransduction in vascular endothelial cells [23]. Conversely, transient mechanoactivation has been shown to generate ceramides by rearranging enzymatic activities in caveolae [40]. We have recently shown that mechanosensing alters the dynamic movements of TM cells via cytoskeletal remodeling [17, 18]. Cytoskeletal remodeling of TM cells allows calibration of AH outflow through the TM filter, and membrane lipid rearrangements are likely to be an integral part of such remodeling process.

As mentioned above, transient mechanotransduction rearranges sphingomyelin-ceramide conversion enzymatic activities in caveolae [40]. Caveolae are lipid “rafts” organized into membrane microdomains in association with sphingolipids and cholesterols [47]. Single nucleotide polymorphisms in genes for cell membrane integral protein caveolin 1 (CAV-1) and caveolin 2 (CAV-2) have been identified as genetic risk factors strongly associated with glaucoma [48]. The caveolae, besides playing a mechanosensing role, also harbors nitric oxide synthase (NOS) [49], cycloxygenase 2 (COX-2) [37], and prostacyclin synthase (PGIS) [50], the later ones are known players in IOP regulation.

The early pathology in glaucoma is likely to be a transition from ocular normotensive to hypertensive state. While normal AH can be derived from human subjects undergoing cataract surgery, and glaucomatous AH subjected to various medication or prior surgical intervention can also be collected, ethical reasons generally forbid collection of AH from human ocular hypertensives individuals without subjecting them to any prior treatment. The collection of AH from hypertensive individuals without subjecting them any intervention first is considered unethical thus necessitating the use of animal models for such analyses. DBA/2J mice [51] remain one of the suitable rodent models [52] that presents a spontaneous elevation in IOP in contrast to most other animal models. DBA/2J enables studying AH composition in normotensive and hypertensive states and thus helps capture lipid/metabolites associated with each of these states. In DBA/2J mice, the IOP elevation and development of glaucoma is natural, age-related, variable, progressive and asynchronous [24, 25]. The ocular hypertension in DBA/2J is generally thought to be due to pigmentary dispersion [53]. However, as noted above the IOP elevation in DBA/2J is somewhat

asynchronous, thus different mice development IOP elevation at somewhat different age and to a different degree. Our in vivo non-invasive microscopic and optical coherence tomography (OCT) imaging, IOP measurement has revealed lack of correlation between elevation in IOP and pigmentary dispersion. The lack of correlation between IOP elevation and pigmentary dispersion has also been further corroborated by Fontana-Masson staining of the anterior chamber tissue as endpoint analyses post IOP measurement (unpublished observations). DBA/2J mice therefore allow analyses of metabolites from normotensive and hypertensive tissues in those animals where the iridocorneal angle remains open, which were evaluated by non-invasive OCT imaging. It is pertinent to note that in human subjects, pigment dispersion does not always correlate with elevated IOP, furthermore such pigmentary materials often clear up without inducing IOP elevation [54].

There is an overall reduction in total lipids from the normotensive state to the hypertensive state (Fig. 3A), however, sphingomyelin and sphingoid bases show a reduction in total amount, while S1Ps and ceramides show an increase from normotensive to hypertensive states (Fig. 3B-E). Of all four classes analyzed here, total S1Ps underwent the greatest change in total lipid amounts followed by sphingomyelins, where both were found to be statistically significant as DBA/2J mice reached a hypertensive state (Fig. 3D, 3B). Irrespective of gender, both female and male mice show an overall reduction in total lipids when analyzed separately (Fig. 4A). The reduced amount of sphingomyelin and sphingoid base and increased amount of S1Ps and ceramides from the normotensive to hypertensive states occur across both genders similarly. The differences in total amounts from normotensive to hypertensive for sphingoid base species in males were found to be statistically significant (Fig. 4B). Human diseases caused by impaired metabolism of sphingolipids and ceramides are generally due to defects in enzymes that degrade these lipids [55]. Our data suggests that the levels of lipids are altered in the hypertensive state compared to normotensive state, which could potentially be associated with altered levels or biological activities of the enzymes involved in their metabolism (Fig. 1). Changes in phospholipids with concomitant changes in enzymatic activities have been found in the TM [32]. Significant phospholipid changes were also found in the AH between normal control and glaucomatous human subjects [12], which could potentially attributed to altered enzymatic activities for these lipids in the TM as noted above and possibly in other surrounding tissues as well. Whether activity of key enzymes in the sphingolipid pathway are also impaired in transition from normotensive to a hypertensive state remains to be investigated.

In our current study we found several sphingolipids and ceramides that are unique to the normotensive and hypertensive states 17 and 34 species respectively (Tables 2-3). In DBA/2J females and males, 30 and 28 sphingomyelin species were found as common, respectively, between normotensive and hypertensive states (Supplementary Tables S1-S2). In DBA/2J males and females, 27 and 28 sphingoid base species were found as common, respectively, between normotensive and hypertensive states (Supplementary Tables S1-S2). Only 6 and 5 S1P species were found as common in males and females, respectively, between normotensive and hypertensive states (Supplementary Tables S1-S2). Finally, 40 and 43 ceramides were found as common, respectively, between normotensive and hypertensive states (Supplementary Tables S1-S2).

Four common lipid species: sphingolipid base analog, iso (4E,15-methyl-d16:1) sphingosine, C16 sphinganine Sphinganine-1-phosphate, Phytosphingosine 1-phosphate (PhS1P) and SM(d17:1/24:1), showed a ≥5 fold change in amount in the AH between normotensive and hypertensive states. The sphingolipid base analog, iso (4E,15-methyl-d16:1) sphingosine is likely involved in cell survival, cell growth and proliferation and related physiological processes [56], C16 sphinganine Sphinganine-1-phosphate level changes has been noted with fumonisin B_1toxicity [57]. Fumonisins are fungal lipids that may occur in the anterior eye tissue either from local infection/commensalism or assimilated from contaminated food [58]. They structurally mimic sphingoid bases and act as competitive inhibitors of sphingolipid biosynthesis and metabolism [58-61]. PhS1P has been recently implicated in cellular stress responses in yeast [62], and also act as a high affinity ligand for the $S1P_4$ receptors [63] and may potentially be involved in cell signaling [64, 65]. The SM(d17:1/24:1) is a ceramide phosphocholine analog that may potentially play a role in tissue injury, infection and inflammation [66].

Cer(d18:0/18:1(9Z)) was found in to be uniquely expressed in female DBA/2J mice in the normotensive phase (Table 3) and was previously identified as unique in human control AH [11]. Ceramides have a variety of functions, ranging from precursors for glycosphingolipids and gangliosides to the induction of the apoptotic pathway [67]. Because Cer(d18:0/18:1(9Z)) disappears in the glaucomatous AH in humans and in the hypertensive phase in female DBA/2J mice, it suggests that Cer(d18:0/18:1(9Z)) potentially has a function in the regulation of AH outflow. We postulate that the ceramide species is either part of some aberrant signaling pathway resulting in the increased production of AH or decreased outflow. Another possibility is that the ceramide species is sequestered in the TM upon IOP elevation and subsequent pathology associated with IOP elevation. Further investigations will show the function of Cer(d18:0/18:1(9Z)) and its role in IOP elevation. Cer(d18:0/24:1(15Z)) was found to be unique in both female and male DBA/2J mice in the hypertensive phase when compared to the normotensive state (Tables 2-3) and was found to be unique in the TM of normotensive DBA/2J male mice [25]. The appearance of Cer(d18:0/24:1(15Z)) in normotensive TM and in hypertensive AH suggests that IOP elevation leads to the ceramide species being released from the TM to the AH or that it was sequestered in the AH. Previous studies show that Cer(d18:0/24:1(15Z)) is also present in human glaucomatous AH [11]. Cer(d18:0/24:1(15Z)) is involved with a variety of functions from cell stability and integrity to signaling and energy storage (Supplementary Table S4). Further investigations will reveal its role in IOP elevation pathology.

In summary, we have shown a reduction in total amount of sphingolipids and ceramides (protein normalized values) for all four classes in the DBA/2J AH of hypertensive state compared to normotensive state. A majority of sphingolipids and ceramides are common between normotensive and hypertensive states. However, a number of sphingolipid and ceramide species were found to be uniquely present in normotensive, but absent in hypertensive AH and vice versa. Very little information is available about the specific biological activity and relevance to AH outflow of these unique or common lipids. Further investigation will provide a more in depth understanding of the role of these lipid entities and their contribution in mechanisms of the AH outflow regulation. Similar fold changes have been observed in our previous studies of sphingolipids and ceramides human AH [11].

However, a cohesive understanding as to the exact role of sphingolipids and ceramides in glaucoma pathology is still elusive. We postulate that the modulation of enzymatic pathway (Fig. 1) relating to sphingolipid metabolism may alter the overall levels of sphingolipids and ceramides in the mice concomitant with progression to a hypertensive state. Investigations into the relationship between protein, lipids and enzymatic activities in this pathway remain the next logical step in gaining an understanding of glaucoma pathology. Our results presented here are likely to spark an interest for further studies in identified sphingolipid and ceramide species and their role in glaucoma pathology.

Supplementary Material

Refer to Web version on PubMed Central for supplementary material.

Acknowledgments

This work was partly supported by NIH grants EY016112, P30-EY14801, the Computational Ocular Genomics Training Grant T32EY023194-01 (to GE), and a Research to Prevent Blindness (RPB) unrestricted grant to University of Miami. The TSQ Quantum Access Max procurement was supported by Department of Defense Grant W81XWH-09-1-0674. We thank Mitchell Martinez and Dr. Ayman Aljohani for assistance with the mass spectrometry and collection of aqueous humor respectively.

References

[1]. Morrison, JC.; Acott, TS. Anatomy and physiology of aqueous humor outflow. In: Morrison, JC.; Pollack, IP., editors. Glaucoma Science and Practice. Thieme Medical Publishers Inc.; New York: 2003. p. 34-41.

[2]. Mark HH. Aqueous humor dynamics in historical perspective. Surv Ophthalmol. 2010; 55:89–100. [PubMed: 19783023]

[3]. Civan MM, Macknight AD. The ins and outs of aqueous humour secretion. Exp Eye Res. 2004; 78:625–631. [PubMed: 15106942]

[4]. Quigley HA, Broman AT. The number of people with glaucoma worldwide in 2010 and 2020. Br J Ophthalmol. 2006; 90:262–267. [PubMed: 16488940]

[5]. Wan Z, Woodward DF, Stamer WD. Endogenous Bioactive Lipids and the Regulation of Conventional Outflow Facility. Expert Rev Ophthalmol. 2008; 3:457–470. [PubMed: 19381354]

[6]. Rao PV. Bioactive Lysophospholipids: Role in Regulation of Aqueous Humor Outflow and Intraocular Pressure in the Context of Pathobiology and Therapy of Glaucoma. J Ocul Pharmacol Ther. 2013:181–190. [PubMed: 24283588]

[7]. Ambache N. Irin, a smooth-muscle contracting substance present in rabbit iris. J Physiol. 1955; 129:65–66. [PubMed: 13264154]

[8]. Ambache N. Properties of irin, a physiological constituent of the rabbit's iris. J Physiol. 1957; 135:114–132. [PubMed: 13398970]

[9]. Cracknell KP, Grierson I. Prostaglandin analogues in the anterior eye: their pressure lowering action and side effects. Exp Eye Res. 2009; 88:786–791. [PubMed: 18930047]

[10]. Winkler NS, Fautsch MP. Effects of Prostaglandin Analogues on Aqueous Humor Outflow Pathways. J Ocul Pharmacol Ther. 2013; 30:102–109. [PubMed: 24359106]

[11]. Aljohani A, Munguba GC, Guerra Y, Lee RK, Bhattacharya SK. Sphingolipids and Ceramides of Human Aqueous Humor. Mol Vis. 2013; 19:1966–1984. [PubMed: 24068864]

[12]. Edwards G, Aribindi K, Guerra Y, Lee RK, Bhattacharya SK. Phospholipid profiles of control and glaucomatous human aqueous humor. Biochimie. 2014; 101:232–247. [PubMed: 24561385]

[13]. Aribindi K, Guerra Y, Piqueras MC, Banta JT, Lee RK, Bhattacharya SK. Cholesterol and Glycosphingolipids of Human Trabecular Meshwork and Aqueous humor: Comparative Profiles

from control and glaucomatous donors. Curr Eye Res. 2013; 38:1017–1026. [PubMed: 23790057]

[14]. Bhattacharya SK. Recent advances in shotgun lipidomics and their implication for vision research and ophthalmology. Curr Eye Res. 2013; 38:417–427. [PubMed: 23330842]

[15]. Yang K, Cheng H, Gross RW, Han X. Automated lipid identification and quantification by multidimensional mass spectrometry-based shotgun lipidomics. Anal Chem. 2009; 81:4356–4368. [PubMed: 19408941]

[16]. Stamer WD. The cell and molecular biology of glaucoma: mechanisms in the conventional outflow pathway. Invest Ophthalmol Vis Sci. 2012; 53:2470–2472. [PubMed: 22562843]

[17]. Goel M, Sienkiewicz AE, Picciani R, Lee RK, Bhattacharya SK. Cochlin induced TREK-1 co-expression and annexin A2 secretion: role in trabecular meshwork cell elongation and motility. PLoS One. 2011; 6:e23070. [PubMed: 21886777]

[18]. Goel M, Sienkiewicz AE, Picciani R, Wang J, Lee RK, Bhattacharya SK. Cochlin, intraocular pressure regulation and mechanosensing. PLoS One. 2012; 7:e34309. [PubMed: 22496787]

[19]. Hannun YA, Obeid LM. Principles of bioactive lipid signalling: lessons from sphingolipids, Nature reviews. Molecular cell biology. 2008; 9:139–150. [PubMed: 18216770]

[20]. Snook CF, Jones JA, Hannun YA. Sphingolipid-binding proteins. Biochim Biophys Acta. 2006; 1761:927–946. [PubMed: 16901751]

[21]. Berchtold D, Piccolis M, Chiaruttini N, Riezman I, Riezman H, Roux A, Walther TC, Loewith R. Plasma membrane stress induces relocalization of Slm proteins and activation of TORC2 to promote sphingolipid synthesis. Nat Cell Biol. 2012; 14:542–547. [PubMed: 22504275]

[22]. Berchtold D, Walther TC. TORC2 plasma membrane localization is essential for cell viability and restricted to a distinct domain. Mol Biol Cell. 2009; 20:1565–1575. [PubMed: 19144819]

[23]. Czarny M, Schnitzer JE. Neutral sphingomyelinase inhibitor scyphostatin prevents and ceramide mimics mechanotransduction in vascular endothelium. Am J Physiol Heart Circ Physiol. 2004; 287:H1344–1352. [PubMed: 15142848]

[24]. John SW, Hagaman JR, MacTaggart TE, Peng L, Smithes O. Intraocular pressure in inbred mouse strains. Invest Ophthalmol Vis Sci. 1997; 38:249–253. [PubMed: 9008647]

[25]. Guerra Y, Aljohani AJ, Edwards G, Bhattacharya SK. A Comparison of Trabecular Meshwork Sphingolipids and Ceramides of Ocular Normotensive and Hypertensive States of DBA/2J Mice. J Ocul Pharmacol Ther. 2013:283–290. [PubMed: 24320088]

[26]. Bligh EG, Dyer WJ. A rapid method of total lipid extraction and purification. Can J Biochem Physiol. 1959; 37:911–917. [PubMed: 13671378]

[27]. Bradford MM. A rapid and sensitive method for the quantitation of microgram quantities of protein utilizing the principle of protein-dye binding. Anal Biochem. 1976; 72:248–254. [PubMed: 942051]

[28]. Crane AM, Hua HU, Coggin AD, Gugiu BG, Lam BL, Bhattacharya SK. Mass spectrometric analyses of phosphatidylcholines in alkali-exposed corneal tissue. Invest Ophthalmol Vis Sci. 2012; 53:7122–7130. [PubMed: 22956606]

[29]. Han X, Yang K, Gross RW. Multi-dimensional mass spectrometry-based shotgun lipidomics and novel strategies for lipidomic analyses. Mass Spectrom Rev. 2011; 31:134–178. [PubMed: 21755525]

[30]. Han X. Multi-dimensional mass spectrometry-based shotgun lipidomics and the altered lipids at the mild cognitive impairment stage of Alzheimer's disease. Biochim Biophys Acta. 2010; 1801:774–783. [PubMed: 20117236]

[31]. Pluskal T, Castillo S, Villar-Briones A, Oresic M. MZmine 2: modular framework for processing, visualizing, and analyzing mass spectrometry-based molecular profile data. BMC Bioinformatics. 2010; 11:395. [PubMed: 20650010]

[32]. Aribindi K, Guerra Y, Lee RK, Bhattacharya SK. Comparative Phospholipid Profiles of Control and Glaucomatous Human Trabecular Meshwork. Invest Ophthalmol Vis Sci. 2013; 54:3037–3044. [PubMed: 23557733]

[33]. Benjamin A, Kashem M, Cohen C, Caldwell Busby JA, Salgado-Commissariat D, Helekar SA, Bhattacharya SK. Proteomics of the nucleus ovoidalis and field L brain regions of zebra finch. J Proteome Res. 2008; 7:2121–2132. [PubMed: 18361516]

[34]. Goel M, Picciani RG, Lee RK, Bhattacharya SK. Aqueous humor dynamics: a review. The open ophthalmology journal. 2010; 4:52–59. [PubMed: 21293732]

[35]. Clark R, Nosie A, Walker T, Faralli JA, Filla MS, Barrett-Wilt G, Peters DM. Comparative genomic and proteomic analysis of cytoskeletal changes in dexamethasone-treated trabecular meshwork cells. Mol Cell Proteomics. 2013; 12:194–206. [PubMed: 23105009]

[36]. Fautsch MP, Howell KG, Vrabel AM, Charlesworth MC, Muddiman DC, Johnson DH. Primary trabecular meshwork cells incubated in human aqueous humor differ from cells incubated in serum supplements. Invest Ophthalmol Vis Sci. 2005; 46:2848–2856. [PubMed: 16043859]

[37]. Toris CB, Gabelt BT, Kaufman PL. Update on the mechanism of action of topical prostaglandins for intraocular pressure reduction. Surv Ophthalmol. 2008; 53(Suppl1):S107–S120. [PubMed: 19038618]

[38]. Sumida GM, Stamer WD. Sphingosine-1-phosphate enhancement of cortical actomyosin organization in cultured human Schlemm's canal endothelial cell monolayers. Invest Ophthalmol Vis Sci. 2010; 51:6633–6638. [PubMed: 20592229]

[39]. Sumida GM, Stamer WD. S1P(2) receptor regulation of sphingosine-1-phosphate effects on conventional outflow physiology. Am J Physiol Cell Physiol. 2011; 300:C1164–1171. [PubMed: 21289286]

[40]. Czarny M, Liu J, Oh P, Schnitzer JE. Transient mechanoactivation of neutral sphingomyelinase in caveolae to generate ceramide. J Biol Chem. 2003; 278:4424–4430. [PubMed: 12473648]

[41]. Zeidan YH, Hannun YA. The acid sphingomyelinase/ceramide pathway: biomedical significance and mechanisms of regulation. Curr Mol Med. 2010; 10:454–466. [PubMed: 20540705]

[42]. Mondal M, Mesmin B, Mukherjee S, Maxfield FR. Sterols are mainly in the cytoplasmic leaflet of the plasma membrane and the endocytic recycling compartment in CHO cells. Mol Biol Cell. 2009; 20:581–588. [PubMed: 19019985]

[43]. Gault CR, Obeid LM, Hannun YA. An overview of sphingolipid metabolism: from synthesis to breakdown. Adv Exp Med Biol. 2010; 688:1–23. [PubMed: 20919643]

[44]. Ogretmen B, Hannun YA. Biologically active sphingolipids in cancer pathogenesis and treatment. Nature reviews. Cancer. 2004; 4:604–616.

[45]. Luberto C, Yoo DS, Suidan HS, Bartoli GM, Hannun YA. Differential effects of sphingomyelin hydrolysis and resynthesis on the activation of NF-kappa B in normal and SV40-transformed human fibroblasts. J Biol Chem. 2000; 275:14760–14766. [PubMed: 10799564]

[46]. Mettu PS, Deng PF, Misra UK, Gawdi G, Epstein DL, Rao PV. Role of lysophospholipid growth factors in the modulation of aqueous humor outflow facility. Invest Ophthalmol Vis Sci. 2004; 45:2263–2271. [PubMed: 15223804]

[47]. Surgucheva I, Surguchov A. Expression of caveolin in trabecular meshwork cells and its possible implication in pathogenesis of primary open angle glaucoma. Mol Vis. 2011; 17:2878–2888. [PubMed: 22128235]

[48]. Wiggs JL, Kang JH, Yaspan BL, Mirel DB, Laurie C, Crenshaw A, Brodeur W, Gogarten S, Olson LM, Abdrabou W, DelBono E, Loomis S, Haines JL, Pasquale LR. Common variants near CAV1 and CAV2 are associated with primary open-angle glaucoma in Caucasians from the USA. Hum Mol Genet. 2011; 20:4707–4713. [PubMed: 21873608]

[49]. Awadalla MS, Thapa SS, Hewitt AW, Craig JE, Burdon KP. Association of eNOS polymorphisms with primary angle-closure glaucoma. Invest Ophthalmol Vis Sci. 2013; 54:2108–2114. [PubMed: 23422825]

[50]. Spisni E, Bianco MC, Griffoni C, Toni M, D'Angelo R, Santi S, Riccio M, Tomasi V. Mechanosensing role of caveolae and caveolar constituents in human endothelial cells. J Cell Physiol. 2003; 197:198–204. [PubMed: 14502559]

[51]. Libby RT, Anderson MG, Pang IH, Robinson ZH, Savinova OV, Cosma IM, Snow A, Wilson LA, Smith RS, Clark AF, John SW. Inherited glaucoma in DBA/2J mice: pertinent disease features for studying the neurodegeneration. Vis Neurosci. 2005; 22:637–648. [PubMed: 16332275]

[52]. Pang IH, Clark AF. Rodent models for glaucoma retinopathy and optic neuropathy. J Glaucoma. 2007; 16:483–505. [PubMed: 17700292]

[53]. Anderson MG, Smith RS, Hawes NL, Zabaleta A, Chang B, Wiggs JL, John SW. Mutations in genes encoding melanosomal proteins cause pigmentary glaucoma in DBA/2J mice. Nat Genet. 2002; 30:81–85. [PubMed: 11743578]

[54]. Epstein DL, Boger WP 3rd, Grant WM. Phenylephrine provocative testing in the pigmentary dispersion syndrome. Am J Ophthalmol. 1978; 85:43–50. [PubMed: 619685]

[55]. Pralhada Rao R, Vaidyanathan N, Rengasamy M, Mammen Oommen A, Somaiya N, Jagannath MR. Sphingolipid metabolic pathway: an overview of major roles played in human diseases. J Lipids. 2013:178910. [PubMed: 23984075]

[56]. Smith ER, Merrill AH, Obeid LM, Hannun YA. Effects of sphingosine and other sphingolipids on protein kinase C. Methods Enzymol. 2000; 312:361–373. [PubMed: 11070884]

[57]. Menaldino DS, Bushnev A, Sun A, Liotta DC, Symolon H, Desai K, Dillehay DL, Peng Q, Wang E, Allegood J, Trotman-Pruett S, Sullards MC, Merrill AH Jr. Sphingoid bases and de novo ceramide synthesis: enzymes involved, pharmacology and mechanisms of action. Pharmacol Res. 2003; 47:373–381. [PubMed: 12676511]

[58]. Aljohani AJ, Edwards G, Guerra Y, Dubovy S, Miller D, Lee RK, Bhattacharya SK. Human Trabecular Meshwork Sphingolipid and Ceramide Profiles and Potential Latent Fungal Commensalism. Invest Ophthalmol Vis Sci. 2014; 55:3413–3422. [PubMed: 24787569]

[59]. Sforza S, Dall'asta C, Marchelli R. Recent advances in mycotoxin determination in food and feed by hyphenated chromatographic techniques/mass spectrometry. Mass Spectrom Rev. 2006; 25:54–76. [PubMed: 15892148]

[60]. Paepens C, De Saeger S, Van Poucke C, Dumoulin F, Van Calenbergh S, Van Peteghem C. Development of a liquid chromatography/tandem mass spectrometry method for the quantification of fumonisin B1, B2 and B3 in cornflakes. Rapid Commun Mass Spectrom. 2005; 19:2021–2029. [PubMed: 15973649]

[61]. Zachariasova M, Lacina O, Malachova A, Kostelanska M, Poustka J, Godula M, Hajslova J. Novel approaches in analysis of Fusarium mycotoxins in cereals employing ultra performance liquid chromatography coupled with high resolution mass spectrometry. Anal Chim Acta. 2010; 662:51–61. [PubMed: 20152265]

[62]. Cowart LA, Shotwell M, Worley ML, Richards AJ, Montefusco DJ, Hannun YA, Lu X. Revealing a signaling role of phytosphingosine-1-phosphate in yeast. Mol Syst Biol. 2010; 6:349. [PubMed: 20160710]

[63]. Candelore MR, Wright MJ, Tota LM, Milligan J, Shei GJ, Bergstrom JD, Mandala SM. Phytosphingosine 1-phosphate: a high affinity ligand for the S1P(4)/Edg-6 receptor. Biochem Biophys Res Commun. 2002; 297:600–606. [PubMed: 12270137]

[64]. Meyer zu Heringdorf D, Jakobs KH. Lysophospholipid receptors: signalling, pharmacology and regulation by lysophospholipid metabolism, Biochim. Biophys Acta. 2007; 1768:923–940.

[65]. Lee JP, Cha HJ, Lee KS, Lee KK, Son JH, Kim KN, Lee DK, An S. Phytosphingosine-1-phosphate represses the hydrogen peroxide-induced activation of c-Jun N-terminal kinase in human dermal fibroblasts through the phosphatidylinositol 3-kinase/Akt pathway. Arch Dermatol Res. 2012; 304:673–678. [PubMed: 22566145]

[66]. Thompson D, Pepys MB, Wood SP. The physiological structure of human C-reactive protein and its complex with phosphocholine. Structure. 1999; 7:169–177. [PubMed: 10368284]

[67]. Tserng KY, Griffin RL. Ceramide metabolite, not intact ceramide molecule, may be responsible for cellular toxicity. Biochem J. 2004; 380:715–722. [PubMed: 14998372]

Highlights

- Sphingolipid & ceramide profiles of DBA/2J mouse aqueous humor were analyzed.
- Quantitative differences between normotensive to hypertensive states were compared.
- Mass spectrometry showed several sphingolipid species common between each state.
- Selected lipids were uniquely present in normotensive or in hypertensive state.
- A decrease in total amount of lipids was found in hypertensive state.

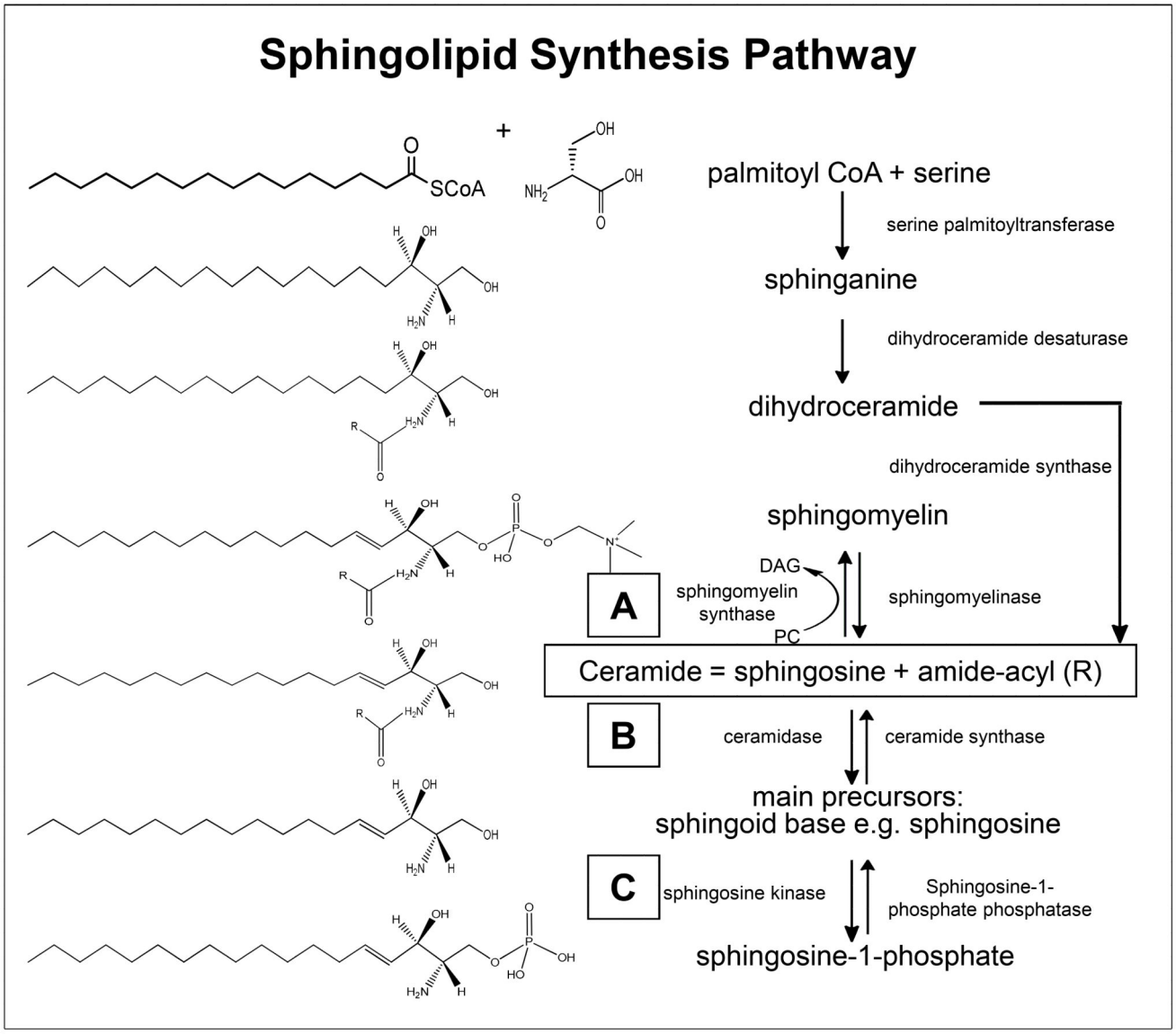

Fig. 1.

Schematic depiction of sphingolipid metabolism pathway. Sphingolipids are synthesized de novo from serine plus palmitoyl CoA. Serine palmitoyltransferase catalyses the breakdown of serine plus palmitoyl CoA to sphinganine. Acylation of sphinganine by the enzyme dihydroceramide desaturase to produce dihydroceramide occurs and the final reaction to produce ceramide is catalyzed by dihydroceramide synthase. Ceramide undergoes one of three fates: (a) addition of headgroups to generate sphingomyelins, (b) glycosphingolipids and, (c) cleavage to sphingosine leading to sphingosine-1-phosphate. Boxed letters A, B and C indicate the location of the enzyme(s) in the overall scheme of metabolism responsible for conversion of indicated lipid species. Our identified lipid species and their potential conversion enzymes in these specific locations in the scheme have been indicated in Table 4 and Supplementary Table S3.

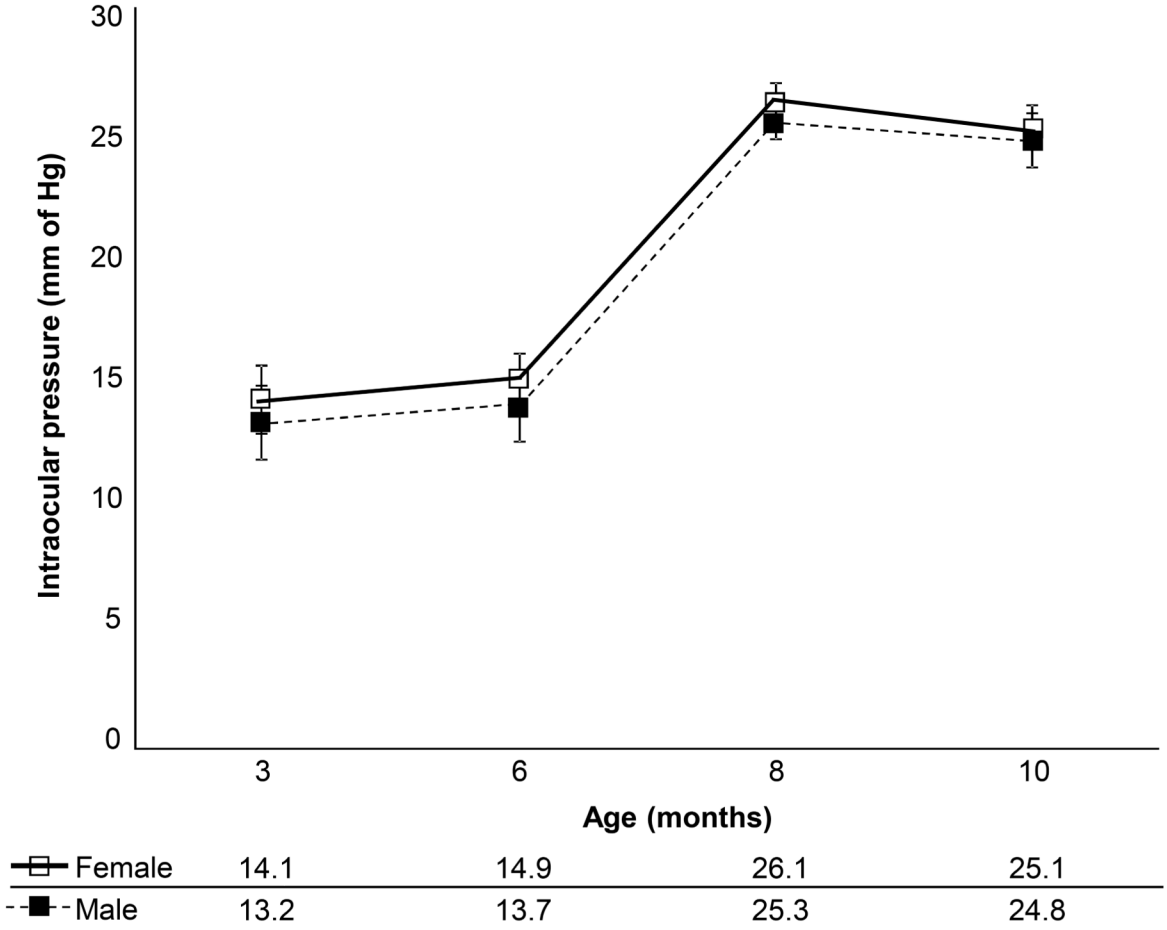

Fig. 2.

Intraocular pressure (IOP) profile. IOP measurements for both genders of DBA/2J mice determined using a TonoLab instrument. Age of the animal at the time of tissue collection and IOP in mm of Hg is as indicated. Average IOP and standard deviation from a week of twice daily measurements have been indicated for each age and gender. Each group contained n=40 animals.

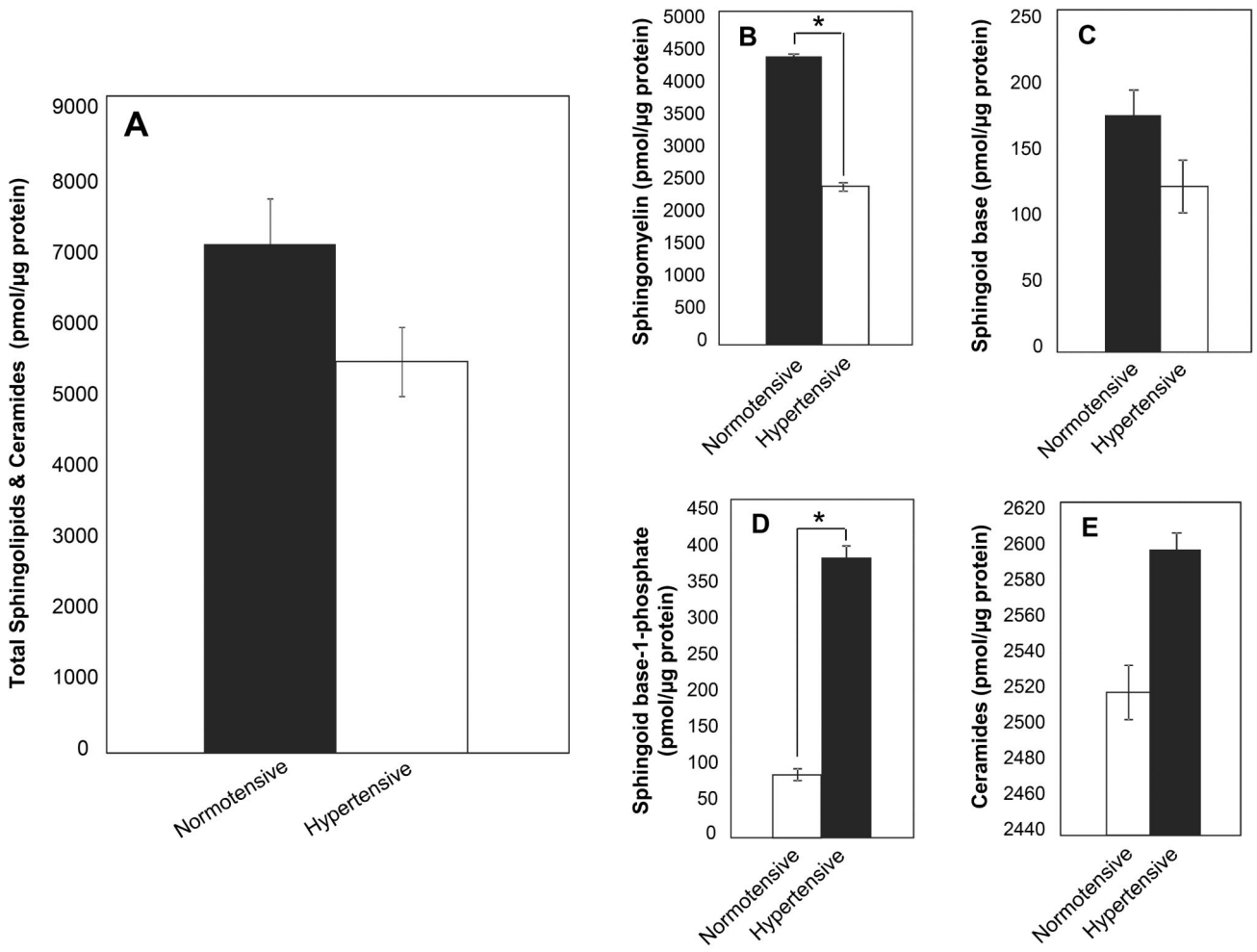

Fig. 3.

(A) Comparison of average total amounts of sphingolipids and ceramides for normotensive and hypertensive states of both genders combined. Estimated average total amount of (B) sphingomyelin, (C) sphingoid base, (D) S1P and (E) ceramides in normotensive and hypertensive states are represented as filled and hollow bar graphs [(*p<0.05), differences are relative to the normotensive state].

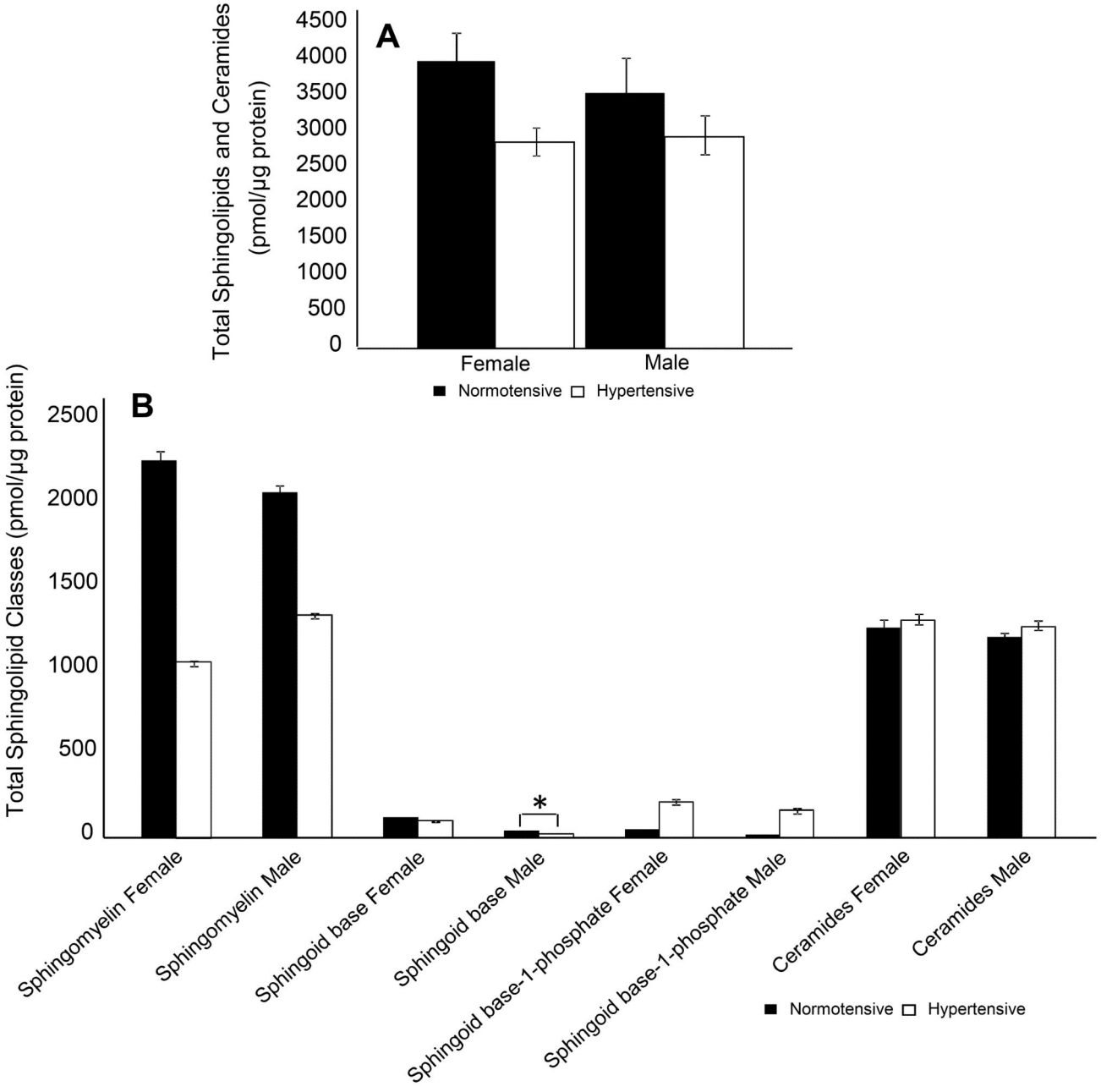

Fig. 4.

(A) Estimated average total amounts of sphingolipids and ceramides for normotensive and hypertensive states between both genders. Comparison of average total amounts of (B) sphingolipid classes between normotensive and hypertensive states are represented as filled and hollow bar graphs[(*p<0.05), differences are relative to the normotensive state].

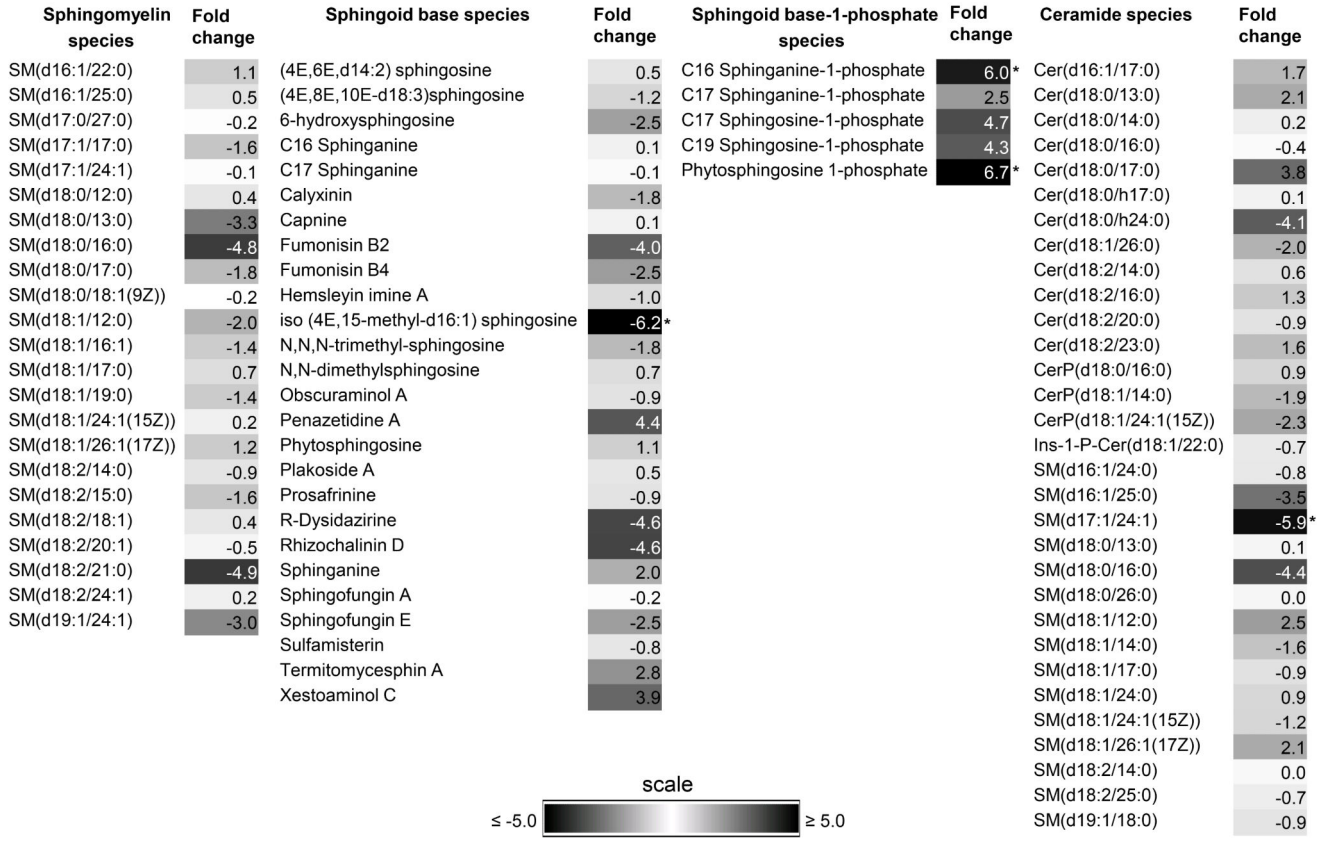

Fig. 5.

Heat map of fold change (fc) in common lipid species between normotensive and hypertensive states of both genders combined. The fold change is the ratio relative to normotensive state based on a $\log_2$ scale. A negative sign precedes before modulus where the denominator is higher indicating higher amounts are present in normotensive than hypertensive state. Scale bar of fc used for given lipid species are as indicated[*|fc|≥ 5.0].

Table 1
Parameters and internal standards for analyses of different sphingolipids classes

Lipid Class	Name of the lipid standard	Parent Mass	Ion Mode	Daughter Mass (m/z)	CE (V)	Scan Type	Catalog Number*
Sphingomyelin	N-oleoyl-D-erythro-sphingosylphosphorylcholine	729.1	+	213.2	50	NLS	860587
Sphingoid base	D-erythro-sphingosine	299.5	+	48.0	18	NLS	860490
Sphingoid base-1-phosphate	D-erythro-sphingosine-1-phosphate	379.5	−	79.1	24	PIS	860402
Ceramide	N-oleoyl-D-erythro-sphingosine	563.9	−	256.2	32	NLS	860519

*All standards were procured from Avanti polar Lipids, Albaster, AL unless stated otherwise. NLS= neutral loss scan; PIS= Precursor ion scan. CE= collision energy in volts.

Table 2

Unique Sphingolipid and Ceramide Species in Normotensive and Hypertensive Female DBA/2J Aqueous Humor

Lipid Species[a]	Theoretical m/z[b]	m/z	Error (Da)	Average lipid amount (pmol per species/μg protein)[c]	LIPIDMAPS ID	PUBCHEM ID	HMDB Accession[d]
Sphingomyelin							
Normotensive Aqueous Humor							
SM(d16:1/16:0)[e]	675.5	676.0	0.5	2.9	LMSP03010035	123068746	
SM(d16:0/22:0)	761.7	762.2	0.5	19.4	LMSP03010063	123068774	
Hypertensive Aqueous Humor							
SM(d18:1/20:1)[e]	757.6	758.0	0.4	244.3	LMSP03010059	123068770	
SM(d18:0/22:0)	789.7	790.1	0.4	3.6	LMSP03010022	7850656	
SM(d16:1/20:1)[e]	729.6	730.2	0.6	0.5	LMSP03010048	123068759	
SM(d16:0/20:0)	733.6	734.3	0.7	36.7	LMSP03010053	123068764	
SM(d18:0/24:0)	817.7	818.1	0.4	15.1	LMSP03010024	7850658	
SM(d18:1/22:1)	785.7	786.5	0.8	71.6	LMSP03010072	123068783	
Sphingoid base							
Normotensive Aqueous Humor							
(4E,8Z,d18:2) sphingosine[e]	298.3	297.4	−0.9	2.1	LMSP01080011	74382660	
Hypertensive Aqueous Humor							
Penaresidin A[e]	330.3	330.3	0.0	0.1	LMSP01080045	74382694	
Sphingoid base-1-phosphate							
Normotensive Aqueous Humor							
Sphinganine-phosphate	380.3	380.8	0.5	53.9	LMSP01050002	7850620	HMDB01383

Lipid Species[a]	Theoretical m/z[b]	m/z	Error (Da)	Average lipid amount (pmol per species/μg protein)[c]	LIPIDMAPS ID	PUBCHEM ID	HMDB Accession[d]
C16 Sphingosine-1-phosphate	350.2	350.7	0.5	2.1	LMSP01050005	123068722	
Ceramides							
Normotensive Aqueous Humor							
Cer(d18:0/18:1(9Z))	564.5	565.2	0.7	3.4	LMSP02020015	49703627	HMDB11763
Cer(d18:1/18:1(9Z))	562.5	563.3	0.8	0.1	LMSP02010003	4266351	HMDB04948
SM(d18:0/12:0)[e]	647.5	648.4	0.9	0.2	LMSP03010079	123068790	
SM(d18:0/15:0)[e]	689.6	690.4	0.8	1.8	LMSP03010091	123068802	
Hypertensive Aqueous Humor							
SM(d18:0/17:0)[e]	717.6	718.6	1.0	4.0	LMSP03010046	123068757	
SM(d16:1/18:0)[e]	701.6	702.4	0.8	0.1	LMSP03010042	123068753	
SM(d16:1/20:1)[e]	727.6	728.5	0.9	0.1	LMSP03010048	123068759	
SM(d18:1/20:0)	757.6	758.4	0.8	0.1	LMSP03010005	7850648	
SM(d18:2/22:1)	781.6	781.9	0.3	7.5	LMSP03010070	123068781	
Cer(d18:0/24:1(15Z))	648.6	649.6	1.0	4.1	LMSP02020011	7850635	HMDB11769
SM(d16:1/22:1)	755.6	755.3	−0.3	4.0	LMSP03010058	123068769	
SM(d18:0/20:0)	759.6	760.4	0.8	0.1	LMSP03010021	7850655	
SM(d18:0/24:0)	815.7	816.4	0.7	35.0	LMSP03010024	7850658	
SM(d18:1/15:0)[e]	687.5	688.4	0.9	0.1	LMSP03010038	123068749	
SM(d18:2/21:0)	769.6	769.1	−0.6	4.1	LMSP03010064	123068775	

[a] The lipid species identification is based on Lipidmaps database, customized and used as a .csv file for bioinformatic analyses with the MZmine 2.9 program.

[b] The theoretical mass by charge ratio (m/z) presented is in positive ion mode [M+H]+ for sphingomyelin and sphingoid base. Whereas negative ion mode [M-H]− has been presented for sphingoid base-1-phosphate and ceramide. Error in Da has been provided from theoretical data.

[c] Average standard normalized dataset is presented here. Species that are known bonafide lipids of non-mammalian origin were excluded. However, where the origin in mammalian or human is unclear those entities were retained.

[d]The only lipids species in this table found to have an HMDB identifier (HMDB01383, HMDB11763, HMDB04948, HMDB11769), the following details have been reported: Localization: cytoplasm, extracellular, membrane, endoplasmic reticulum. Functions: cell signaling, component of glycosphingolipid metabolism, fuel and energy storage, fuel or energy source, membrane integrity/stability, component of glycerolipid metabolism, component of glycerophospholipid metabolism,component of prostaglandin and leukotriene metabolism, and second messenger.

[e]Lipids common to females and males.

Table 3

Unique Sphingolipid and Ceramide Species in Normotensive and Hypertensive Male DBA/2J Aqueous Humor

Lipid Species[a]	Theoretical m/z[b]	m/z	Error (Da)	Average lipid amount (pmol per species/μg protein)[c]	LIPIDMAPS ID	PUBCHEM ID	HMDB Accession[d]
Sphingomyelin							
Normotensive Aqueous Humor							
SM(d18:0/15:0)[e]	691.6	691.9	0.3	6.9	LMSP03010091	123068802	
SM(d20:0/24:1)	843.7	843.2	−0.5	1.7	LMSP03010088	123068799	
Hypertensive Aqueous Humor							
SM(d16:1/16:0)[e]	675.5	675.5	−0.1	12.2	LMSP03010035	123068746	
SM(d18:1/22:0)	787.7	787.2	−0.5	239.8	LMSP03010006	7850649	
SM(d16:1/17:0)	689.6	689.9	0.3	1.5	LMSP03010037	123068748	
SM(d16:1/20:1)[e]	729.6	729.3	−0.3	0.7	LMSP03010048	123068759	
SM(d17:1/22:0)	773.7	773.8	0.1	23.0	LMSP03010066	123068777	
SM(d18:0/14:0)	677.6	676.6	−1.0	6.2	LMSP03010030	49703632	
SM(d18:0/24:1(15Z))	815.7	815.7	0.0	18.9	LMSP03010023	7850657	
SM(d18:1/20:1)[e]	757.6	756.6	−1.0	19.8	LMSP03010059	123068770	
Sphingoid base							
Hypertensive Aqueous Humor							
Penaresidin A[e]	330.3	330.3	0.0	1.2	LMSP01080045	74382694	
Ceramides							
Normotensive Aqueous Humor							
Cer(t18:0/26:0)	694.7	694.8	0.1	7.4	LMSP02030005	85297410	

Lipid Species[a]	Theoretical m/z[b]	m/z	Error (Da)	Average lipid amount (pmol per species/μg protein)[c]	LIPIDMAPS ID	PUBCHEM ID	HMDB Accession[d]
CerP(d18:1/24:0)	728.6	727.7	−0.9	1.4	LMSP02050008	7850645	HMDB10704
SM(d16:1/18:0)[e]	701.6	702.3	0.8	2.7	LMSP03010042	123068753	
SM(d18:1/15:0)[e]	687.5	687.9	0.4	5.1	LMSP03010038	123068749	
SM(d18:1/16:1)	699.5	700.0	0.5	7.2	LMSP03010041	123068752	
SM(d18:2/15:0)	685.5	686.2	0.7	1.9	LMSP03010036	123068747	
Hypertensive Aqueous Humor							
Cer(d18:1/22:0)	620.6	621.2	0.6	0.5	LMSP02010008	7850626	HMDB04952
SM(d16:1/20:1)[e]	727.6	728.1	0.5	7.8	LMSP03010048	123068759	
SM(d16:1/24:1)	783.6	784.3	0.6	0.2	LMSP03010071	123068782	
SM(d18:0/12:0)[e]	647.5	648.1	0.6	6.0	LMSP03010079	123068790	
SM(d18:0/18:1(9Z))	729.6	730.1	0.5	0.1	LMSP03010031	49703633	
SM(d18:0/26:1(17Z))	841.7	842.3	0.6	0.1	LMSP03010025	7850659	
Cer(d16:1/22:0)	592.6	593.2	0.7	13.0	LMSP02010016	123068725	
Cer(d18:0/24:1(15Z))	648.6	649.3	0.7	0.1	LMSP02020011	7850635	HMDB11769
Cer(d18:1/18:1(9Z))	562.5	563.3	0.8	47.0	LMSP02010003	4266351	HMDB04948
Cer(d18:1/26:1(17Z))	674.6	675.6	1.0	2.0	LMSP02010010	7850628	HMDB04954
SM(d18:0/17:0)[e]	717.6	718.1	0.5	2.9	LMSP03010046	123068757	
SM(d18:1/25:0)	827.7	828.1	0.4	2.7	LMSP03010027	49703629	

[a] The lipid species identification is based on Lipidmaps database, customized and used as a .csv file for bioinformatic analyses with the MZmine 2.9 program.

[b] The theoretical mass by charge ratio (m/z) presented is in positive ion mode [M+H]+ for sphingomyelin and sphingoid base. Whereas negative ion mode [M-H]− has been presented for sphingoid base-1-phosphate and ceramide. Error in Da has been provided from theoretical data.

[c] Average standard normalized dataset is presented here. Species that are known bonafide lipids of non-mammalian origin were excluded. However, where the origin in mammalian or human is unclear those entities were retained.

[d] The only lipids species in this table that was found to have an HMDB identifier (HMDB10704, HMDB04952, HMDB11769, HMDB04948, HMDB04954), following details have been reported: Localization: extracellular membrane and membrane component, functions: membrane integrity, cell signaling, energy source and energy storage.

[e] Lipids common to females and males.

Table 4

Identified Unique Lipid Species and their integration with the Sphingolipid Synthesis Pathway

Boxed Letter	Lipid Name	Gender	State
A (Sphingomyelinase, Sphingomyelin synthase)	SM(d16:1/16:0)	Female/Male	Normotensive
	SM(d16:0/22:0)	Female	Normotensive
	SM(d18:1/20:1)	Female/Male	Hypertensive
	SM(d18:0/22:0)	Female	Hypertensive
	SM(d16:1/20:1)	Female/Male	Hypertensive
	SM(d16:0/20:0)	Female	Hypertensive
	SM(d18:0/24:0)	Female	Hypertensive
	SM(d18:1/22:1)	Female	Hypertensive
	SM(d18:0/15:0)	Female/Male	Normotensive
	SM(d20:0/24:1)	Male	Normotensive
	SM(d16:1/16:0)	Female/Male	Hypertensive
	SM(d18:1/22:0)	Male	Hypertensive
	SM(d16:1/17:0)	Male	Hypertensive
	SM(d16:1/20:1)	Female/Male	Hypertensive
	SM(d17:1/22:0)	Male	Hypertensive
	SM(d18:0/14:0)	Male	Hypertensive
	SM(d18:0/24:1(15Z))	Male	Hypertensive
	SM(d18:1/20:1)	Female/Male	Hypertensive
B (Ceramidase, Ceramide synthase)	Cer(d18:0/18:1(9Z))	Female	Normotensive
	Cer(d18:1/18:1(9Z))	Female	Normotensive
	SM(d18:0/12:0)	Female/Male	Normotensive
	SM(d18:0/15:0)	Female/Male	Normotensive
	SM(d18:0/17:0)	Female/Male	Hypertensive
	SM(d16:1/18:0)	Female/Male	Hypertensive
	SM(d16:1/20:1)	Female/Male	Hypertensive
	SM(d18:1/20:0)	Female	Hypertensive
	SM(d18:2/22:1)	Female	Hypertensive
	Cer(d18:0/24:1 (15Z))	Female	Hypertensive

Boxed Letter	Lipid Name	Gender	State
	SM(d16:1/22:1)	Female	Hypertensive
	SM(d18:0/20:0)	Female	Hypertensive
	SM(d18:0/24:0)	Female	Hypertensive
	SM(d18:1/15:0)	Female/Male	Hypertensive
	SM(d18:2/21:0)	Female	Hypertensive
	Cer(t18:0/26:0)	Male	Normotensive
	CerP(d18:1/24:0)	Male	Normotensive
	SM(d16:1/18:0)	Female/Male	Normotensive
	SM(d18:1/15:0)	Female/Male	Normotensive
	SM(d18:1/16:1)	Male	Normotensive
	SM(d18:2/15:0)	Male	Normotensive
	Cer(d18:1/22:0)	Male	Hypertensive
	SM(d16:1/20:1)	Female/Male	Hypertensive
	SM(d16:1/24:1)	Male	Hypertensive
	SM(d18:0/12:0)	Female/Male	Hypertensive
	SM(d18:0/18:1(9Z))	Male	Hypertensive
	SM(d18:0/26:1(17Z))	Male	Hypertensive
	Cer(d16:1/22:0)	Male	Hypertensive
	Cer(d18:0/24:1 (15Z))	Male	Hypertensive
	Cer(d18:1/18:1(9Z))	Male	Hypertensive
	Cer(d18:1/26:1 (17Z))	Male	Hypertensive
	SM(d18:0/17:0)	Female/Male	Hypertensive
	SM(d18:1/25:0)	Male	Hypertensive
C (Sphingosine kinase, S-1-P phosphatase)	Sphinganine-phosphate	Female	Normotensive
	C16 Sphingosine-1-phosphate	Female	Normotensive
	(4E,8Z,d18:2) sphingosine	Female	Normotensive
	Penaresidin A	Female/Male	Hypertensive
	Penaresidin A	Female/Male	Hypertensive

Letters **A, B** and **C** indicates the location of enzyme responsible for conversion in the schematic sphingolipid synthesis pathway as depicted in Figure 1 for the identified lipid species. Lipids common to females and males have been indicated by Female/Male.